ISBN: 978-3-95450-231-8 ISSN: 2673-5490 doi: 10.18429/JACoW-IPAC2023-THPM035

FIRST HIGH QUALITY DRIFT TUBE LINAC CAVITY ADDITIVELY MANUFACTURED FROM PURE COPPER

M. Mayerhofer[1], J. Mittenender[1], C. Wittig[1], I. Prestes[1], E. Jägle[1] and G. Dollinger[1]
[1]Universität der Bundeswehr München, 85579 Neubiberg, Germany

Abstract

Recently presented RF cavity prototypes printed entirely from pure copper illustrate the potential of additive manufacturing (AM), and particularly laser powder bed fusion (L-PBF), for accelerator technology. Thereby, the design freedom of L-PBF is only limited by overhanging geometries, which have to be printed with supporting structures to ensure sufficient accuracy. However, the subsequent removal of these support structures is a major challenge for cm-sized GHz cavities. Therefore, our approach is to design self-supporting geometries. In this contribution, we present a drift tube cavity geometry as used in e.g. proton therapy linac systems that can be fabricated by L-PBF without support structures. A 5-cell prototype was manufactured from high-purity copper using L-PBF. It is shown that the developed geometry allows a print accuracy sufficient to reach the defined resonance frequency. A chemical, as well as a dynamic electrochemical finishing process, was applied to optimize the prototype's surface quality. Thus, the CST simulated Q_0 was obtained for the first time with a printed copper cavity.

INTRODUCTION

Most linear particle accelerators (linacs) are essentially based on high-frequency cavities (cavities). Due to their complex geometries, cavities are usually assembled from several parts by joining processes, e.g. in several brazing steps [1–3]. This conventional manufacturing process is a major reason why cavities account for a significant portion of the capital cost of accelerator systems. The conventional manufacturing process is also very challenging in terms of freedom of design. To realize an economical or even feasible manufacturing process, the cavity performance (quality factor, cooling capacity, etc.) is often severely compromised. In contrast, additive manufacturing (AM) or colloquially 3D printing allows the manufacturing of complex geometries in one piece, resulting in high-cost efficiency and significantly reduced design restrictions [4]. Recently published prototypes of cavities fully or partially manufactured using AM techniques demonstrate the potential of this approach for accelerator technology. These include among others a radio frequency quadrupole cavity (750 MHz) [5], an interdigital H-mode cavity (433 MHz) [6], and superconducting cavities (up to 6 GHz MHz) [7, 8].

The TM_{010} 3 GHZ drift tube cavity (DTL prototype) we presented in [9] was the first ready-to-use cavity printed entirely from pure copper (see fig. 1). It was manufactured by laser powder bed fusion (L-PBF). The cavity is comparable to the drift tube linac part of the Side Coupled Drift Tube linacs used in proton radiotherapy linac systems [10, 11] and consists of five DTL cells. In L-PBF, overhanging geometries require support structures printed along with them to maintain geometric accuracy, the more the geometry design tends to the horizontal. Subsequent removal of support structures is very complex or often not possible in cm-sized GHz cavities. Our approach is, therefore, to design cavities with self-supporting, overhanging structures ("arch profiles"), to maintain print quality (compare red marked regions fig. 2). In vacuum testing, a pressure of $2 \cdot 10^{-7}$ mbar was achieved without bake out procedure with standard vacuum equipment. The measured resonant frequency (f_R) of (3000 ± 1) MHz deviates slightly from the f_R of 2998 MHz simulated by CST Microwave Studio® (CST). Variations like this can be corrected with standard tuning devices such as variable tuning rods (see fig. 1) and also occur in the conventional manufacturing process. The unloaded quality factor (Q_0) of 8750 ± 10 is reduced by about 33 % compared to the CST simulation (13017). This reduction is mainly due to the high inner surface roughness (plane arithmetic mean height S_a) of more than 10 µm compared to the skin depth of $\delta \approx 1.2$ µm. In the following, we show that the simulated Q_0 is achieved after post-processing the cavity with an electrochemical/chemical post-processing named Hirtisation® [12].

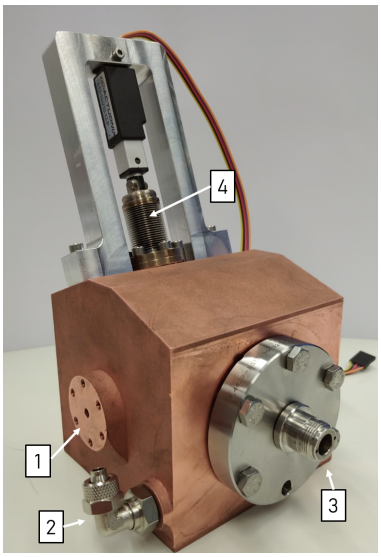

Figure 1: Printed 3 GHz DTL cavity with: 1) Bore, 2) Cooling valves, 3) Couple loop and 4) Variable tuner

ISBN: 978-3-95450-231-8 ISSN: 2673-5490 doi: 10.18429/JACoW-IPAC2023-THPM035

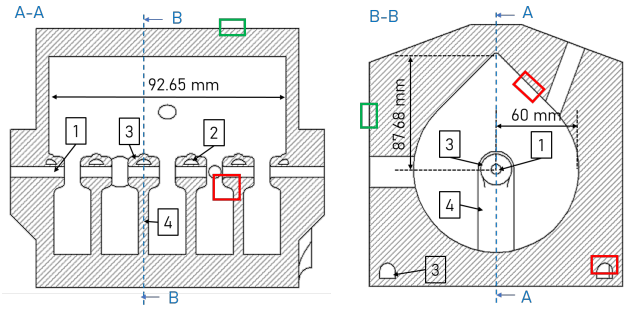

Figure 2: Longitudinal and cross section of the self supporting cavity with bore (1), cooling valves (2), drift tubes (3) and stems (4). Marked in Red: Self supporting overhanging sections. In green: Location of Roughness measurement.

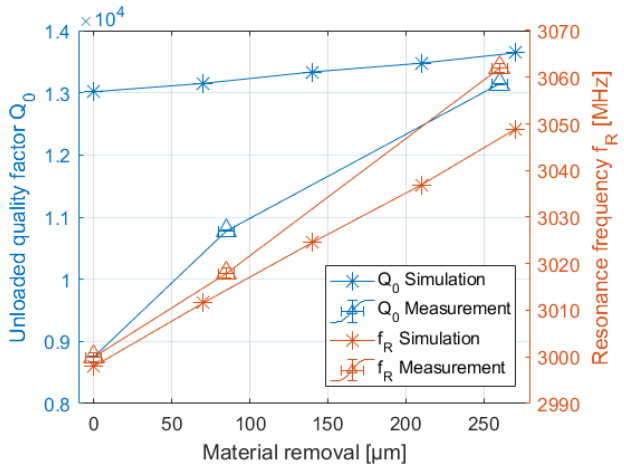

Figure 3: Evaluation of Q_0 and f_R as a function of the material removal by Hirtisation®. Measured values are marked with a △, simulated values with a ∗.

EVALUATION OF THE DTL PROTOTYPE

Due to the dimensions of the DTL prototype, the internal surface roughness cannot be reduced by machining. Instead, processes such as conventional or chemically assisted surface mass finishing, mechanical-physical-catalyst surface treatments, or chemical and electrochemical processes are an option. In our case, the DTL prototype was finished by means of Hirtisation® [12], a process patented by RENA®. For pure copper and the DTL prototype geometry, Hirtisation® is a combination of chemical and dynamic electrochemical processes based on the liquid media Cu-Auxilex and Cu-Delevatex. This process allows the surface treatment and removal of powder remains even in narrow and deep hollows.

We performed two independent Hirtisation® runs. The material removal during the first and second runs corresponded to approx. 85 µm and 175 µm, respectively.

Figure 3 shows the change in resonant frequency f_R and unloaded quality factor Q_0 in dependence on material removal. f_R and Q_0 are measured using a vector network analyzer (Siglent SNA5002A) via the coupling loop (see fig. 1) and are marked with a △. The corresponding quantities as simulated with CST are marked with ∗. A Q_0 of 13139 ± 10 was measured after the second Hirtisation® run. This corresponds to approx. 96.3 % of the simulated Q_0. Since the simulated Q_0 is never fully achieved in conventional manufacturing due to e.g. geometrical deviations, it can be said that the cavity has achieved a quality comparable to conventionally manufactured cavities. f_R has increased by 64 MHz due to material removal. The change in f_R can be accounted for in future designs in order to achieve the targeted f_R.

In addition to the dependence of unloaded quality factor Q_0, figure 4 shows the change of surface roughness (plane arithmetic mean height S_a) in dependence of material removal. $S_{a\ ISO\ 4288}$ was determined following the ISO 4288 standard. $S_{a\ 100\ \mu m}$ was evaluated as $S_{a\ ISO\ 4288}$ but with an additional high-pass filter for wavelengths greater than 100 µm. $S_{a\ ISO\ 4288}$ as well as $S_{a\ 100\ \mu m}$ were measured at the green marked areas (see fig. 2) using the optical 3D measuring system Alicona Infinitive Focus SL.

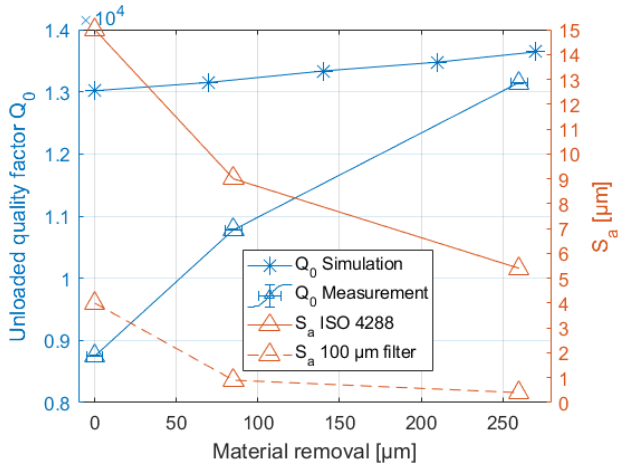

Figure 4: Evaluation of Q_0 and S_a as a function of the material removal. The △ mark the measured values, simulated values are marked with ∗.

A $S_{a\ ISO\ 4288}$ of 5.4 µm and a $S_{a\ 100\ \mu m}$ of 0.4 µm results after the second Hirtisation® run and therefore after a material removal of approx. 260 µm.

In conventional cavity manufacturing, the target rms surface roughness R_q is usually well below δ. This requirement is derived from models such as the Hammerstad Model (HM), which describes the increase in surface resistivity as a function of R_q for small δ respectively high radio frequency signals [13, 15]. For a resonant frequency of 3 GHz and $R_q = \delta \approx 1.2$ µm, the HM predicts an increase in surface resistance of approx. 60 %. The resulting reduction of Q_0 is not easy to predict because the current direction is not always perpendicular to the greatest roughness. However, it is usually well above 20 % [13, 14]. Nevertheless, we reach

ISBN: 978-3-95450-231-8 ISSN: 2673-5490 doi: 10.18429/JACoW-IPAC2023-THPM035

the simulated Q_0 although R_q according to ISO 4288 is still 6.97 µm after the second Hirtisationrun.

In conventional machining, surface roughness is mainly composed of: 1. A more or less prominent low-frequency waviness, depending on the quality of the machine. 2. Many long grooves are created by the roughness profile of the tool itself and occur at a high repetition frequency. In order to measure the "true roughness" at e.g. R_q = 2 - 10 µm, ISO 4288, demands a cut-off wavelength of 2.5 mm to eliminate the waviness. The HM is based on the assumption that the high-frequency current must follow the surface profile perpendicular to these grooves (imposing an “indirection”), which leads to a reduction in conductivity [16]. Obviously, this principle is suitable in the case of long grooves resulting from a tool profile but not in the case of AM-manufactured post-processed workpieces. Figure 5 shows that in this case surface roughness is dominated by local (roundish) defects (powder residues, holes, etc.) which may have much less influence on the current flow than long grooves [16]. Eventually, the HM can be used if a medium-frequency waviness is filtered out by a reduction of the cut-off wavelength. For example, for a cut-off wavelength of 100 µm, the R_q is 0.76 µm. Alternatively, one could try to evaluate the influence of roughness on conductivity in the AM case using 3-D models of hemispherical surface roughness as described in [17]. However, the requirements for surface roughness Q_0 resulting from the experience of conventional cavity manufacturing cannot currently be transferred to additively manufactured cavities such as those presented here.

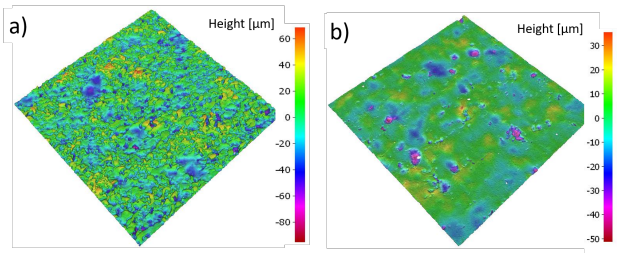

Figure 5: Surface roughness before (a) and after (b) the two Hirtisation® runs.

The E-field distribution of the TM_{010} -mode of the DTL prototype was evaluated after post-processing using a bead-pulling test bench [18]. Figure 6 shows the E-field distribution as a function of the bead position on the beam axis, $|\vec{E}_0(z)|$ normalized to the power loss of the cavity $\sqrt{P}$. The geometric accuracy of the unit cell length of the DTL prototype can be evaluated based on the variation of the distances and amplitude of the E-field maxima between the drift tubes. The position accuracy of the bead is 0.08 mm. Therefore, the measurement uncertainty of the distances can be stated as 0.113 mm. The distances between the maxima are equal within the measurement uncertainty. However, a more accurate assessment of the manufacturing accuracy is intended after the bead-pulling test bench has been further optimised. The measured mean value of the unit cell length is (18.59 ± 0.06) mm which is in good agreement to the design value of 18.53 mm. The amplitude variation is less than (2.9 ± 0.4) %. Therefore, the geometric accuracy would be sufficient in the first order to use the presented 3 GHz cavity as part of a proton radiotherapy linac system as presented in [10, 11].

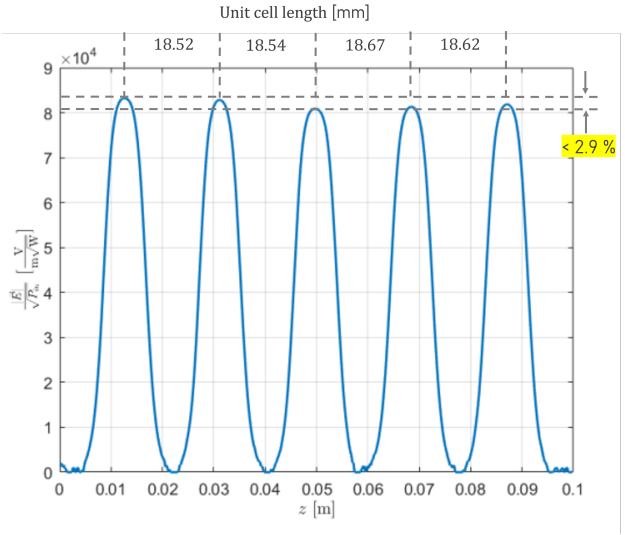

Figure 6: Electric field distribution along the beam axis ($|\vec{E}(z)|$) as measured for the fundamental TM_{010} -mode.

CONCLUSION

A drift tube linac prototype additively manufactured entirely from high-purity copper using L-PBF was post-processed by a chemical- electrochemical process called Hirtisation® [12]. We showed that the simulated quality factor Q_0 is (virtually) achieved after a material removal of approx. 260 µm. This removal of material corresponds to the roughness of $S_{a\ ISO\ 4288}$ of 5.4 µm and a $S_{a\ 100\ \mu m}$ of 0.4 µm which is significantly greater than the roughness required in conventional manufacturing to achieve the simulated Q_0. We are therefore of the opinion that a roughness parameter or a correction factor needs to be established to link surface roughness and Q_0 in the AM case. The E-field distribution and geometric accuracy were fundamentally analysed. The geometric variations are comparable to conventionally manufactured cavities as they are already used in Linac systems today. Our work shows for the first time that additive manufactured GHz cavities can achieve the simulated Q_0 by suitable post-processing procedures. Despite the post-processing, the manufacturing costs are still lower by a factor of 3 compared to a comparable traditionally manufactured cavity [19]. Our next goal is to test the high gradient properties of structures manufactured by the presented methods.

REFERENCES

[1] I.H. Wilson, "Cavity construction techniques", In Proc. CERN Accelerator School of RF Engineering for Particle Accelerators, Oxford, Uk, Apr. 1991, CERN 92-03, vol. 2, doi: 10.5170/CERN-1992-003.

ISBN: 978-3-95450-231-8 ISSN: 2673-5490 doi: 10.18429/JACoW-IPAC2023-THPM035

[2] A. Nassiri et al., "History and technology developments of radio frequency (RF) systems for particle accelerators", IEEE Transactions on Nuclear Science, Institute of Electrical and Electronics Engineers (IEEE), New Jersey, US, Apr. 2016, vol. 63, no. 2 pp. 707–750, doi: 10.1109/TNS.2015.2485164.

[3] S.R. Ghodke et al., "Machining and brazing of accelerating RF cavity", In Proc. 2014 International Symposium on Discharges and Electrical Insulation in Vacuum (ISDEIV), Mumbai, India, US, Oct. 2014, pp. 101-104, doi: 10.1109/DEIV.2014.6961629.

[4] F. Calignano et al., "Overview on Additive Manufacturing Technologies", In Proc. IEEE, Institute of Electrical and Electronics Engineers (IEEE), New Jersey, US, Apr. 2017, vol. 105, no. 4. pp. 593-612, doi: 10.1109/JPROC.2016.2625098.

[5] T. Torims et al., "Evaluation of geometrical precision and surface roughness quality for the additively manufactured radio frequency quadrupole prototype", Journal of Physics: Conference Series. Institute of Physics (IOP) Publishing, Jul. 2023, vol. 2420, No. 1, p. 012089, doi: 10.1088/1742-6596/2420/1/012089.

[6] H. Hähnel et al., "Update on the First 3D Printed IH-Type Linac Structure - Proof-of-Concept for Additive Manufacturing of Linac RF Cavities", In Proc. 31th International Linear Accelerator Conf. (LINAC2022), Liverpool, UK, Jan. 2022, pp. 170–173, doi: 10.18429/JACoW-LINAC2022-MOPOGE11.

[7] S. Jenzer et al., "Prospects of additive manufacturing for accelerators", In Proc. 10th International Particle Accelerator Conf. (IPAC2019), Melbourn, Australia, May. 2019, pp. 4118–4120. doi: 10.18429/JACoW-IPAC2019-THPTS008.

[8] P. Frigola et al., "Advance additive manufacturing method for SRF cavities of various geometries", In Proc. 17th International Conf. on RF Superconductivity (SRF2015), Whistler, Canada, Dec. 2015 pp. 1181–1184, doi: 10.18429/JACoW-SRF2015-THPB042.

[9] M. Mayerhofer et al., "A 3D printed pure copper drift tube linac prototype", Review of Scientific Instruments, American Institute of Physics (AIP) Publishing, Feb. 2022, vol., no. 2, p. 023304, doi: 10.1063/5.0068494.

[10] C. Ronsivalle et al., "The TOP-IMPLART linac: machine status and experimental activity", In Proc. 8th International Particle Accelerator Conference (IPAC2017), Copenhagen, Denmark, May 2017, pp. 4669–4672, doi: 10.18429/JACoW-IPAC2017-THPVA090.

[11] A. Degiovanni et al., "Status of the Commissioning of the LIGHT Prototype", In Proc. 9th International Particle Accelerator Conference (IPAC2018), Vancouver, Canada, May 2018, pp. 425–428, doi: 10.18429/JACoW-IPAC2018-MOPML014.

[12] Rena Technologies GmbH, "Surface Treatment of 3D-Printed Metal Parts", https://www.rena.com/en/technology/process-technology/hirtisation, May 14. 2023.

[13] R.G. Carter, "Microwave and RF vacuum electronic power sources", The Cambridge RF and Microwave Engineering Series, Cambridge University Press, Cambridge, UK, Apr. 2018, vol. 1, pp. 107–109, doi: 10.1017/9780511979231.

[14] A. Hernandez et al., "Resonant cavities for measuring the surface resistance of metals at X-band frequencies", Journal of Physics E: Scientific Instruments, Institute of Physics (IOP) Publishing, Bristol, UK, 1986, vol. 19, no. 3, p. 100, doi: 10.1088/0022-3735/19/3/013.

[15] A.H. Seltzman and S.J. Wukitch, "RF losses in selective laser melted GRCop-84 copper waveguide for an additively manufactured lower hybrid current drive launcher", Fusion Engineering and Design, Elsevier publishing, Amsterdam, Netherlands, Nov. 2020, vol. 159, p. 111762, doi: 10.1016/j.fusengdes.2020.111762.

[16] G. Gold, "A Physical Surface Roughness Model and Its Applications", IEEE Transactions on Microwave Theory and Techniques, Institute of Electrical and Electronics Engineers (IEEE), New Jersey, US, May 2017, vol. 65, pp. 3720-3732, doi: 10.1109/TMTT.2017.2695192.

[17] S. Hall et al., "Multigigahertz Causal Transmission Line Modeling Methodology Using a 3-D Hemispherical Surface Roughness Approach", IEEE TRANSACTIONS ON MICROWAVE THEORY AND TECHNIQUES, Institute of Electrical and Electronics Engineers (IEEE), New Jersey, US, Dec. 2007, vol. 55, pp. 2614-2623, doi: 10.1109/TMTT.2007.910076.

[18] C. Wittig, "Entwicklung eines Störkörpermessstandes zur Charakterisierung von Hochfrequenz-Hohlraumresonatoren", Bachelor Thesis, University of the Bundeswehr Munich, Munich, Germany, Mar. 2023, https://www.unibw.de/lrt2/publikationen/thesis.

[19] M. Mayerhofer et al., "Concept and performance evaluation of two 3 GHz buncher units optimizing the dose rate of a novel preclinical proton minibeam irradiation facility", PLOS ONE, Public Library of Science, San Francisco, US, Oct. 2021, vol. 16, p. e0258477, doi: 10.1371/journal.pone.0258477.